models with narrow and intermediate-width slabs (fig. S3, A and B). Such rollback drove the main phase of Basin and Range extension (Fig. 3, G and H).

References and Notes

1. R. M. Russo, P. G. Silver, *Science* **263**, 1105 (1994).
2. M. D. Long, P. G. Silver, *Science* **319**, 315 (2008).
3. G. Zandt, E. Humphreys, *Geology* **36**, 295 (2008).
4. E. Di Giuseppe, J. van Hunen, F. Funiciello, C. Faccenna, D. Giardini, *Geochem. Geophys. Geosyst.* **9**, Q02014 (2008).
5. W. P. Schellart, *Geochem. Geophys. Geosyst.* **9**, Q03014 (2008).
6. C. Kincaid, R. W. Griffiths, *Nature* **425**, 58 (2003).
7. W. P. Schellart, *J. Geophys. Res.* **109** (B7), B07401 (2004).
8. D. R. Stegman, J. Freeman, W. P. Schellart, L. Moresi, D. May, *Geochem. Geophys. Geosyst.* **7**, Q03012 (2006).
9. R. L. Carlson, T. W. C. Hilde, S. Uyeda, *Geophys. Res. Lett.* **10**, 297 (1983).
10. S. Goes, F. A. Capitanio, G. Morra, *Nature* **451**, 981 (2008).
11. P. Molnar, T. Atwater, *Earth Planet. Sci. Lett.* **41**, 330 (1978).
12. R. D. Jarrard, *Rev. Geophys.* **24**, 217 (1986).
13. D. W. Forsyth, S. Uyeda, *Geophys. J. R. Astron. Soc.* **43**, 163 (1975).
14. Materials and methods are available as supporting material on *Science* Online.
15. F. A. Capitanio, G. Morra, S. Goes, *Geochem. Geophys. Geosyst.* **10**, Q04002 (2009).
16. G. Morra, K. Regenauer-Lieb, D. Giardini, *Geology* **34**, 877 (2006).
17. D. R. Stegman, R. Farrington, F. A. Capitanio, W. P. Schellart, *Tectonophysics* **483**, 29 (2010).
18. L. Moresi, M. Gurnis, *Earth Planet. Sci. Lett.* **138**, 15 (1996).
19. R. C. Kerr, J. R. Lister, *J. Geol.* **99**, 457 (1991).
20. W. P. Schellart, J. Freeman, D. R. Stegman, L. Moresi, D. May, *Nature* **446**, 308 (2007).
21. C. Kreemer, W. C. Hammond, *Geology* **35**, 943 (2007).
22. P. G. DeCelles, *Am. J. Sci.* **304**, 105 (2004).
23. L. J. Sonder, C. H. Jones, *Annu. Rev. Earth Planet. Sci.* **27**, 417 (1999).
24. R. G. Gordon, D. M. Jurdy, *J. Geophys. Res.* **91** (B12), 12389 (1986).
25. R. D. Müller, M. Sdrolias, C. Gaina, W. R. Roest, *Geochem. Geophys. Geosyst.* **9**, Q04006 (2008).
26. L. M. Flesch, W. E. Holt, A. J. Haines, B. Shen-Tu, *Science* **287**, 834 (2000).
27. W. R. Buck, *J. Geophys. Res.* **96** (B12), 20161 (1991).
28. W. R. Dickinson, W. S. Snyder, *J. Geol.* **87**, 609 (1979).
29. T. Atwater, *Geol. Soc. Am. Bull.* **81**, 3513 (1970).

30. We appreciate discussions and interactions with R. Kerr, R. Govers, F. Capitanio, S. Zlotnik, M. Sandiford, R. Griffiths, and R. Weinberg. We thank the Victorian Partnership for Advanced Computing, the National Computational Infrastructure, and AuScope for computational resources and technical support. This work was supported by an award under the Merit Allocation Scheme on the National Computational Infrastructure National Facility at the Australian National University. W.P.S. was supported by a QE II Fellowship and Discovery grant DP0771823 from the Australian Research Council, a Monash Fellowship from Monash University, and a J. G. Russell Award from the Australian Academy of Science. D.R.S. was supported in part by a Centenary Research Fellowship from the University of Melbourne and in part by the G. Unger Vetlesen Foundation. L.M. and R.J.F. were supported by Discovery grant DP0878501.

Supporting Online Material

www.sciencemag.org/cgi/content/full/329/5989/316/DC1
Materials and Methods
Figs. S1 to S3
Table S1
References

1 April 2010; accepted 11 June 2010
10.1126/science.1190366

Simulated Rapid Warming of Abyssal North Pacific Waters

Shuhei Masuda,[1]* Toshiyuki Awaji,[2,3] Nozomi Sugiura,[2] John Philip Matthews,[3,4] Takahiro Toyoda,[1] Yoshimi Kawai,[1] Toshimasa Doi,[1] Shinya Kouketsu,[1] Hiromichi Igarashi,[2] Katsuro Katsumata,[1] Hiroshi Uchida,[1] Takeshi Kawano,[1] Masao Fukasawa[1]

Recent observational surveys have shown significant oceanic bottom-water warming. However, the mechanisms causing such warming remain poorly understood, and their time scales are uncertain. Here, we report computer simulations that reveal a fast teleconnection between changes in the surface air-sea heat flux off the Adélie Coast of Antarctica and the bottom-water warming in the North Pacific. In contrast to conventional estimates of a multicentennial time scale, this link is established over only four decades through the action of internal waves. Changes in the heat content of the deep ocean are thus far more sensitive to the air-sea thermal interchanges than previously considered. Our findings require a reassessment of the role of the Southern Ocean in determining the impact of atmospheric warming on deep oceanic waters.

The densest waters of the world's oceans are formed around Antarctica where heat exchange with the atmosphere and subsequent ice formation create uniquely dense water masses that sink rapidly and move northward. This Antarctic Bottom Water (AABW) (*1*, *2*) remains largely isolated from further heat exchange as it spreads over much of the world's ocean floor. By replenishing the supply of AABW, highly productive source regions such as the Weddell and Ross seas (Fig. 1) play an important role in the maintenance of the global thermohaline circulation system.

Recent observational surveys conducted during the World Ocean Circulation Experiment (WOCE) and the WOCE revisit (WOCE_rev) have revealed that the deepest waters of the major oceans have warmed during recent decades (*3*–*5*). This bottom-water warming ranges in magnitude from 0.003° to 0.01°C in the Pacific Ocean over the period 1985 to 1999 (*3*, *6*). Such temporal changes are of particular interest as they can constrain estimates of the variability of abyssal circulation. The latter have implications for large-scale thermohaline transport and thus for the global three-dimensional heat budget that is presently of vital concern (*7*).

Despite its crucial importance, the physical mechanisms governing bottom-water warming are poorly understood because in situ observations are spatially and temporally sporadic. Recently, a highly accurate ocean data assimila-

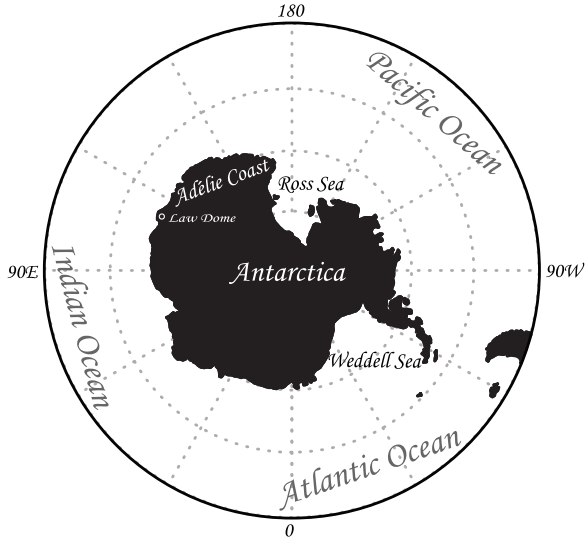

Fig. 1. Antarctic region. The Weddell and Ross seas are major source regions for Antarctic Bottom Water because here the dense, cold, and relatively saline shelf waters formed through air-sea heat exchange sink down the continental slope into the deep Southern Ocean.

[1]Research Institute for Global Change, Japan Agency for Marine-Earth Science and Technology (JAMSTEC), Yokohama 236-0001, Japan. [2]Data Management and Engineering Department, Data Research Center for Marine-Earth Sciences, JAMSTEC, Yokohama 236-0001, Japan. [3]Department of Geophysics, Kyoto University, Kyoto 606-8502, Japan. [4]Environmental Satellite Applications, Llys Awel, Mount Street, Menai Bridge LL595BW, UK.

*To whom correspondence should be addressed. E-mail: smasuda@jamstec.go.jp

tion system has been constructed (*8*), based on a four-dimensional variational (4D-VAR) adjoint approach (*9*, *10*) [supporting online material (SOM)], which can define the mechanism causing an oceanic climate fluctuation by an adjoint sensitivity analysis method that moves the ocean representation backward in time (*11*, *12*) (SOM). We used the "Earth Simulator" supercomputer to perform the major numerical simulations required for this analysis (SOM).

The adjoint sensitivity analysis gives the temporal rate of change of a physical variable in a fixed time and space when model variables (e.g., water temperature, velocity, or surface air-sea fluxes) are arbitrarily changed in the 4D continuum of one temporal and three spatial coordinates. This is equivalent to specifying the "sensitivity" of a variable to small perturbations in the parameters governing the oceanic state (*8*, *13*–*15*). It has been applied to identify the possible causal dynamics, time scales, and pathways involved in the bottom-water warming.

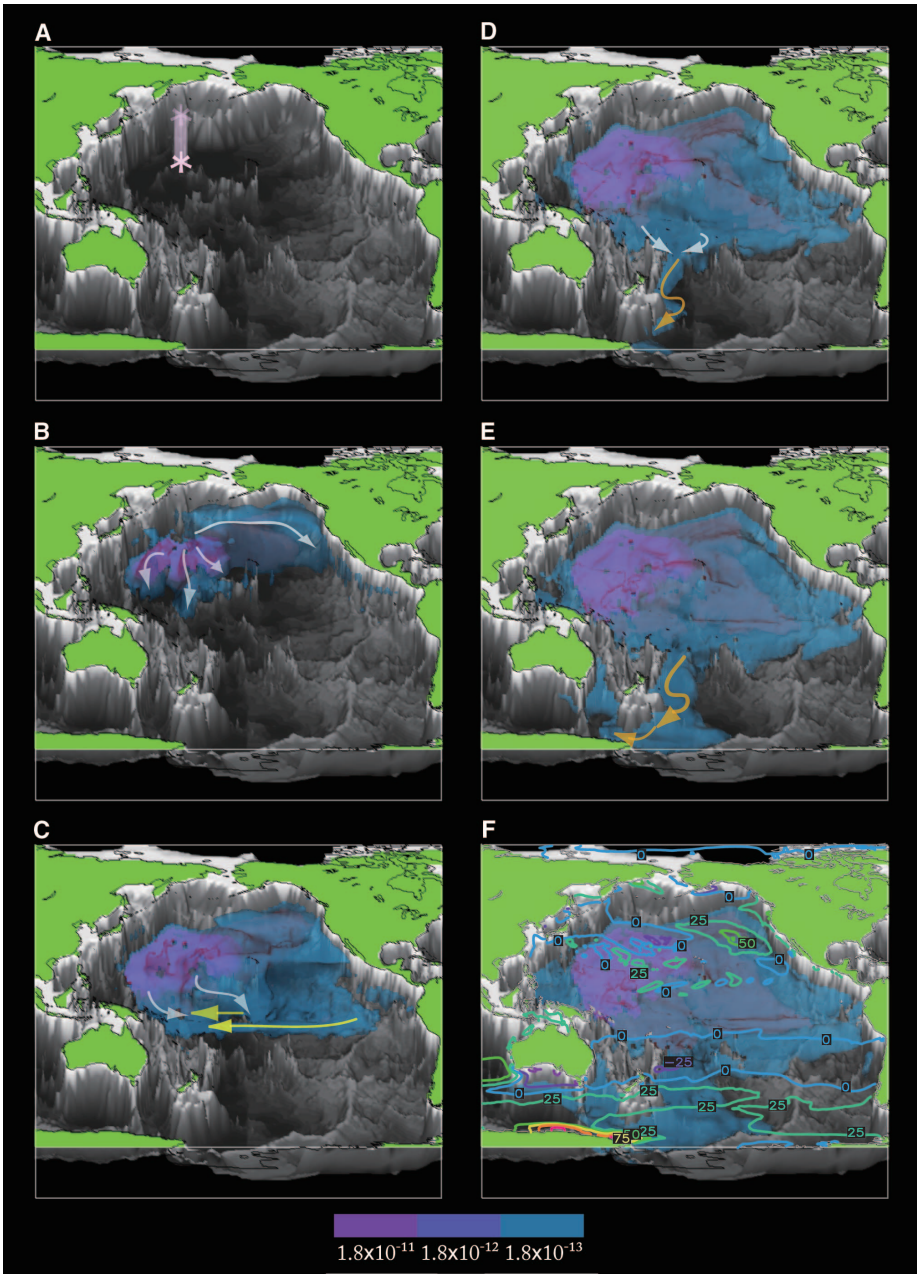

Fig. 2. Bottom-water warming signal identified by an adjoint sensitivity analysis. Temporal rate of change of bottom-water temperature taking place at 47°N-170°E [5200-m depth marked by an asterisk (*) in (A)] in an allocated model time (defined as year zero) when water temperature changes by 1 K in an arbitrary grid point, and showing the pathway of the change in deep-water temperature that will cause the bottom-water warming after (**A**) 0, (**B**) 5, (**C**) 15, (**D**) 25, (**E**) 35, and (**F**) 45 years. The units are dimensionless. Orange and yellow arrows denote the Kelvin and equatorial Rossby wave propagations, respectively. Contours of the temporal rate of change of bottom-water temperature developing at the same location when the net surface air-sea heat flux is steadily changed are traced onto (F). These show the modeled impact of the change in surface air-sea heat flux required to cause the bottom-water warming after 40 years. The units are 1.0×10^{-4} K W^{-1} m^2.

Figure 2 shows the values of the temporal rate of change of bottom-water temperature taking place at 47°N-170°E (5200-m depth) in an allocated model time (defined as year zero) when water temperature changes by 1 K in an arbitrary grid point over a specific time period (in this case, from 0 to −45 years in reverse chronological order). Positive values (indicative of warming in the lowest layer) gradually fill the North Pacific Ocean floor over a 15-year period (Fig. 2, B and C) and then penetrate into the South Pacific through the narrow passage located to the northwest of New Zealand (Fig. 2D). This warming trend can be traced back to the deep Southern Ocean across the Antarctic Circumpolar Circulation region (Fig. 2E) where it then ascends the continental shelf slope around Antarctica. At the end of a 40-year period, the warm signature finally appears at the sea surface in a confined source region that lies off the Adélie Coast (Fig. 2F). The values of the temporal rate of the change, when the net surface air-sea heat flux is changed by 1 W m^{-2} in an arbitrary surface grid point (rather than through a change in water temperature), consistently suggest that the cause of the bottom-water warming in the North Pacific is the increase in the net surface air-sea heat flux into this localized source region (Fig. 2F). (The integrated effect in this region covers 73% of that over the whole Pacific basin, when the values of the temporal rate of the change are effectively assessed with the variance of the heat flux at each surface grid point.) This result implies that a reduction in the volume of AABW due to an increase in the net surface air-sea heat flux in this Southern Ocean region initiates the North Pacific abyssal warming.

Our simulation result reveals a subtle and prompt influence of the Southern Ocean source region on changes in deep-ocean temperature and thus ocean heat budgets. However, the 40-year time scale necessary for these thermal changes to manifest is much shorter than that required by the conventional mechanism, which relies on mass movement (*16*). In the case of an abyssal current flowing northward at a speed of 10^{-3} m s^{-1} (*17*), it would require more than 350 years to cover a distance of 12,000 km.

A more rapid teleconnection between the Southern Ocean surface heating and bottom-water warming in the North Pacific can nevertheless be effected through oceanic internal waves. A thinning of abyssal layers caused by a reduction in AABW formation in a Southern Ocean source region leads to a depression of isopycnal surfaces in the deep ocean (*18*). These isopycnal changes are transmitted as internal oceanic waves, which alter the pressure force

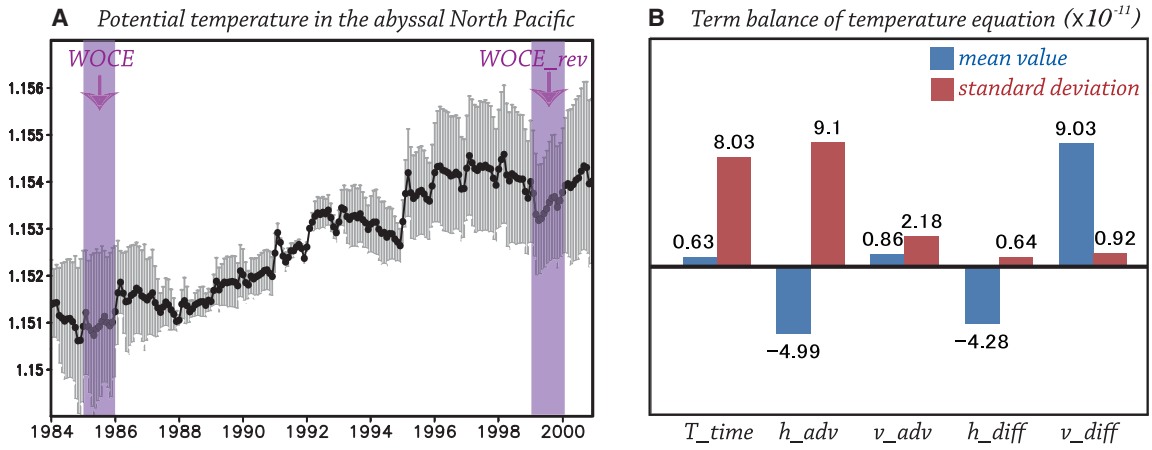

Fig. 3. Bottom-water warming in the synthesized data set. (**A**) Temporal evolution of water temperature from 1984 to 2000 averaged within the North Pacific abyssal basin (155°-170°E, 40°-50°N, 4500- to 5200-m depth). The error bars show the accuracy afforded by the synthesized data set. The units are in kelvin. (**B**) Mean value (blue bar) and standard deviation (red) of each term of the temperature equation averaged over the same abyssal region for the period 1984 to 2000. T_time, local time change; h_adv, horizontal advection; v_adv, vertical advection; h_diff, horizontal diffusion; and v_diff, vertical diffusion. The units are in kelvin per second.

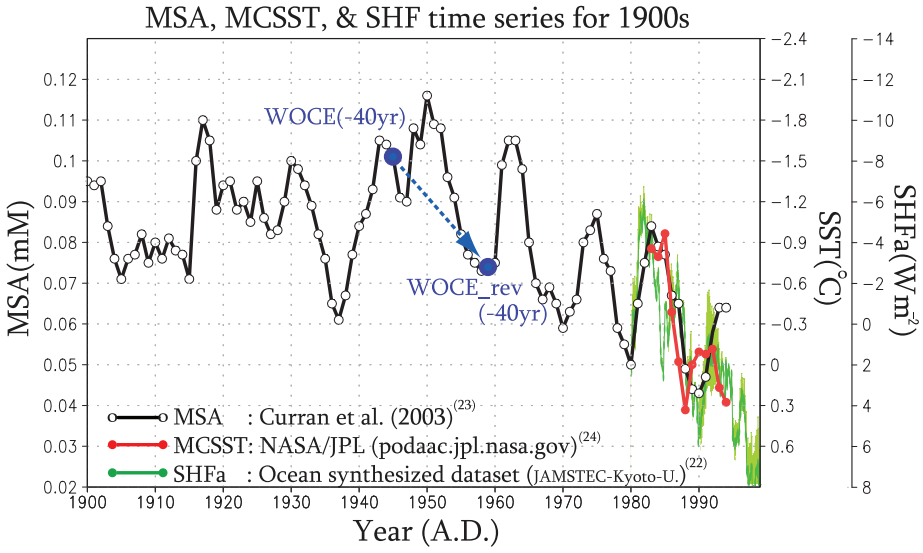

Fig. 4. Evidence of climate change around Antarctica. Law Dome methanesulphonic acid (MSA) record (1900 to 1995; black curve) (*23*), sea surface temperature values (MCSST; for November months during 1982 to 1995; red) (*24*), and estimated downward net surface heat flux anomaly values (SHFa; 1980 to 2000; green) (*22*). The MCSST and SHFa values are averaged over a region off the Adélie Coast (120°E-170°E, 65°S-60°S). The MCSST and SHFa values are plotted with reversed vertical axis. A 3-year running mean has been applied to all the variables. The error bars for the SHFa show the accuracy afforded by the data set. The correlation coefficient value between the MSA and MCSST is 0.73 ($P < 0.01$, $n = 10$), and that between the MSA and SHFa is 0.67 ($P < 0.01$, $n = 13$).

locally and weaken the deep-water current through geostrophic adjustment (*19*, *20*). Bottom-water warming could be then achieved by a reduction in the deep-water current that transports the cool waters of the AABW (*3*).

Internal topographic Kelvin waves are mainly responsible for the rapid transmission of the changes in the Southern Ocean to the equator (orange arrows in Fig. 2, D and E). The Kelvin waves travel along the deep-ocean trench east of New Zealand in a direction for which the lateral boundary is always on the left (in the Southern Hemisphere; SOM). They propagate along the density interfaces of the deep ocean at internal-wave speeds (*21*) of ~7.0×10^{-2} m s^{-1}, corresponding to 2208 km per year (SOM). The signal travels in the opposite direction (with the lateral boundary on the right) in this sensitivity analysis because the calculation moves the ocean representation backward in time.

Internal and topographic Rossby waves are also responsible for the transmission over the undulating bottom topography in the west-central region of the Northern Hemisphere (Fig. 2B). Internal equatorial Kelvin waves, whose (reversed) propagation is identified by the westward equatorially trapped wave track in the deep layers (yellow arrows in Fig. 2C), drive the link between northern and southern hemispheres.

We have examined the proposed mechanism by using a new synthesized ocean data set from 4D-VAR data assimilation (*22*) (SOM). In this synthesized data set, the bottom-water warming is successfully reproduced as a positive temperature trend of ~0.003 K from 1985 to 1999 (between the WOCE and WOCE_rev observational periods) in the North Pacific (Fig. 3A). The term balance of the temperature equation in this abyssal region from the synthesized field (SOM) shows that an overall balance between the horizontal advective and diffusive cooling, and the vertical diffusive heating, is present throughout the period (blue bars in Fig. 3B). The geothermal heating effect is implicitly incorporated in the vertical diffusive heating. Local time change is a subtle positive value, representing the bottom-water warming, as a residual of these major terms. The standard deviation of each term shows that the temporal change in the horizontal advection mainly causes the variations of the local time change (red bars), implying that the changes in the abyssal circulation due to the wave propagations (SOM) constrain the bottom-water warming.

In addition, our results are also consistent with fragmental direct evidence reported in previous observational work. Figure 4A shows the time series of change in methanesulphonic acid (MSA) concentrations within a Law Dome ice core (*23*) obtained from a location near the Adélie Coast (Fig. 1). This MSA record is highly correlated with local sea ice extent and hence should be closely connected with the net surface air-sea heat flux in this region. Indeed, the highly significant correlation between the MSA record and sea surface temperature derived from satellite missions (1981 to 2001) (*24*) underlines this close relation (red curve). Actually, the time change in the net surface air-sea heat flux estimation from the synthesized data set (*22*) is well correlated with that in the MSA record in this region (green curve). Also, the correlative time change in the sea-level anomaly derived from high-precision multisatellite altimetry products possibly further supports the proposed link between the changes in the surface conditions and the supply of AABW (SOM). Again, this is

consistent with a recent reduction in bottom-water formation around Antarctica (*25*).

In this context, our derivation of a 40-year response time implies that the bottom-water warming from 1985 to 1999 in the subarctic North Pacific is linked to the decrease in the MSA value from 1945 to 1959, which corresponds to an increase in the net surface air-sea heat flux off the Adélie Coast. Quantitative diagnosis, based on values of the temporal rate of change of bottom-water temperature when net surface air-sea heat flux is steadily changed (Fig. 2F), shows that an observed bottom-water warming from 0.003 to 0.01 K is equivalent to an increase in the net heat flux from 1.0×10^{-1} to 3.2×10^{-1} W m^{-2} per year into the Southern Ocean off the Adélie Coast (SOM). This net heat flux enhancement is broadly consistent with the relevant decadal increase (3.8×10^{-1} W m^{-2} year^{-1}) from 1945 to 1959, as estimated from the ratio of the MSA values (black curve in Fig. 4) to the net surface heat flux (green curve).

In summary, an increase in the heat input into the Southern Ocean off the Adélie Coast leads to bottom-water warming in the North Pacific on a relatively short time scale (within four decades). A reduction in bottom-water formation off the Adélie Coast due to enhanced heat input leads to a change in the configuration of the isopycnal surfaces through the action of oceanic internal waves and thus determines the pressure forcing over the whole abyssal region of the North Pacific. The consequent reduction in abyssal cooling by the deep-ocean current enables the substantial heating by the vertical diffusion inclusive of the geothermal effect to warm the bottom waters. The propagation speed of the internal waves determines the time scale of this teleconnection. The resulting increase in the integrated heat content can reach 1.2×10^{20} J year^{-1} below 4000-m depth in the Pacific basin.

These results suggest that the present global-change paradigm involving a warming surface regime over an abyssal ocean which, through its very slow response time, can be assumed to be a relatively stable regulator of Earth's climate, must be revisited. Our finding of an invasive and rapid teleconnection between polar surface air-sea heat flux change and distant bottom-water warming indicates that the multicentennial-to-millennial developmental time scales currently envisaged in the predicted oceanic response to climate warming are probably too long.

References and Notes

1. A. W. Mantyla, J. L. Reid, *Deep Sea Res. A* **30**, 805 (1983).
2. A. H. Orsi *et al.*, *Prog. Oceanogr.* **43**, 55 (1999).
3. M. Fukasawa *et al.*, *Nature* **427**, 825 (2004).
4. G. C. Johnson, S. C. Doney, *Geophys. Res. Lett.* **33**, L14614 (2006).
5. M. P. Meredith, A. C. N. Garabato, A. L. Gordon, G. C. Johnson, *J. Clim.* **21**, 3327 (2008).
6. T. Kawano *et al.*, *Geophys. Res. Lett.* **33**, L23613 (2006).
7. S. Levitus *et al.*, *Geophys. Res. Lett.* **32**, L02604 (2005).
8. S. Masuda *et al.*, *Geophys. Res. Lett.* **30**, 1868 (2003).
9. Y. Sasaki, *Mon. Weather Rev.* **98**, 875 (1970).
10. C. Wunsch, *The Ocean Circulation Inverse Problem* (Cambridge Univ. Press, New York, 1996).
11. J. Marotzke *et al.*, *J. Geophys. Res.* **104** (c12), 29529 (1999).
12. A. Köhl, *J. Phys. Oceanogr.* **35**, 1455 (2005).
13. J. Schröter, C. Wunsch, *J. Phys. Oceanogr.* **16**, 1855 (1986).
14. I. Fukumori, T. Lee, B. Cheng, D. Menemenlis, *J. Phys. Oceanogr.* **34**, 582 (2004).
15. A. M. Moore, H. G. Arango, E. Di Lorenzo, A. J. Miller, B. D. Cornuelle, *J. Phys. Oceanogr.* **39**, 702 (2009).
16. W. J. Schmitz Jr., *Rev. Geophys.* **33**, 151 (1995).
17. H. M. van Aken, *The Oceanic Thermohaline Circulation* (Springer, New York, 2006).
18. H. Nakano, N. Suginohara, *J. Geophys. Res.* **107**, 3219 (2002).
19. M. Kawase, *J. Phys. Oceanogr.* **17**, 2294 (1987).
20. N. Suginohara, M. Fukasawa, *J. Oceanogr. Soc. Japan* **44**, 315 (1988).
21. J. Pedlosky, *Ocean Circulation Theory* (Springer, New York, 1996).
22. The details of these data are provided on the DIAS Earth Observation Data Sets Web site (www.jamstec.go.jp/e/medid/dias/kadai/clm/clm_or.html).
23. M. A. J. Curran, T. D. van Ommen, V. I. Morgan, K. L. Phillips, A. S. Palmer, *Science* **302**, 1203 (2003).
24. Multi-channel sea surface temperature data (http://podaac.jpl.nasa.gov/PRODUCTS/p016.html), maintained by NASA Jet Propulsion Laboratory Physical Oceanography Distributed Active Archive Center, Pasadena, CA (2003).
25. S. T. Gille, *Science* **295**, 1275 (2002).

26. We thank Y. Ishikawa and the late I. Kaneko for helpful discussions and Y. Sasaki and Y. Hiyoshi for technical support. This work was supported in part by the Data Integration and Analysis System of the Ministry of Education, Culture, Sports, Science and Technology, Japan (MEXT).

Supporting Online Material

www.sciencemag.org/cgi/content/full/science.1188703/DC1
Materials and Methods
Figs. S1 to S3
References

23 February 2010; accepted 8 June 2010
Published online 24 June 2010;
10.1126/science.1188703
Include this information when citing this paper.

Ocean Warming Slows Coral Growth in the Central Red Sea

Neal E. Cantin,* Anne L. Cohen,* Kristopher B. Karnauskas, Ann M. Tarrant, Daniel C. McCorkle

Sea surface temperature (SST) across much of the tropics has increased by 0.4° to 1°C since the mid-1970s. A parallel increase in the frequency and extent of coral bleaching and mortality has fueled concern that climate change poses a major threat to the survival of coral reef ecosystems worldwide. Here we show that steadily rising SSTs, not ocean acidification, are already driving dramatic changes in the growth of an important reef-building coral in the central Red Sea. Three-dimensional computed tomography analyses of the massive coral *Diploastrea heliopora* reveal that skeletal growth of apparently healthy colonies has declined by 30% since 1998. The same corals responded to a short-lived warm event in 1941/1942, but recovered within 3 years as the ocean cooled. Combining our data with climate model simulations by the Intergovernmental Panel on Climate Change, we predict that should the current warming trend continue, this coral could cease growing altogether by 2070.

Hermatypic corals contribute up to 75% of the calcium carbonate ($CaCO_3$) budget of modern reefs through the process of skeleton building (*1*). Today, rates of $CaCO_3$ production by reef corals, thought to be enhanced by the photosynthetic activities of symbiotic algae (zooxanthellae) (*2*, *3*), far exceed carbonate production rates in the absence of biological activity and ensure that rates of reef accretion exceed natural rates of bioerosion, dissolution, and offshore transport (*4*). For individual corals, rapid rates of skeletal growth are essential for successful recruitment, in order to reach a size refuge from mortality (*5*) and to maximize colony surface area for photosynthesis (*6*).

Predictions based on experimental and field observations indicate that the combined effects of rising temperatures and ocean acidification could increase the frequency of bleaching events and reduce coral calcification by 80% of modern values when atmospheric CO_2 concentrations reach 560 parts per million around 2055 (*7*, *8*, *9*). At this point, if rates of $CaCO_3$ production by corals and other reef calcifiers cannot keep up with rates of erosion, the majority of coral reefs could switch from net accreting to net eroding structures. Elevated temperatures suppress the calcification rates of reef-building corals (*10*) by affecting the relationship between the coral host and its algal symbionts (zooxanthellae). As temperatures rise above threshold summertime values, the photosynthetic capacity of the symbiotic zooxanthellae declines (*11*), reducing the availability of algal-derived photosynthate that fuels light-enhanced calcification (*12*). A prolonged increase of ~1°C or more above historical maximum sea surface temperatures (SSTs)

Woods Hole Oceanographic Institution, Woods Hole, MA 02543, USA.
*These authors contributed equally to this work.

Simulated Rapid Warming of Abyssal North Pacific Waters
Shuhei Masuda *et al.*
Science **329**, 319 (2010);
DOI: 10.1126/science.1188703